

# Inactivation of the Chloroplast ATP Synthase $\gamma$ Subunit Results in High Non-photochemical Fluorescence Quenching and Altered Nuclear Gene Expression in *Arabidopsis thaliana*\*<sup>§</sup>

Received for publication, August 1, 2003, and in revised form, October 22, 2003  
Published, JBC Papers in Press, October 23, 2003, DOI 10.1074/jbc.M308435200

Cristina Dal Bosco<sup>‡</sup>, Lina Lezhneva<sup>‡</sup>, Alexander Biehl<sup>§</sup>, Dario Leister<sup>§</sup>, Heinrich Strotmann<sup>¶</sup>,  
Gerd Wanner<sup>‡</sup>, and Jörg Meurer<sup>‡</sup>||

From the <sup>‡</sup>Ludwig-Maximilians-Universität, Department Biologie I, Botanik, Menzingerstrasse 67, 80638 München, <sup>§</sup>Abteilung für Ertragsphysiologie und Pflanzenzüchtung, Max-Planck-Institut für Züchtungsforschung, Carl-von-Linné Weg 10, 50829 Köln, and <sup>¶</sup>Heinrich-Heine-Universität, Biochemie der Pflanzen, Universitätsstrasse 1, 40225 Düsseldorf, Germany

The nuclear *atpC1* gene encoding the  $\gamma$  subunit of the plastid ATP synthase has been inactivated by T-DNA insertion mutagenesis in *Arabidopsis thaliana*. In the seedling-lethal *dpa1* (deficiency of plastid ATP synthase 1) mutant, the absence of detectable amounts of the  $\gamma$  subunit destabilizes the entire ATP synthase complex. The expression of a second gene copy, *atpC2*, is unaltered in *dpa1* and is not sufficient to compensate for the lack of *atpC1* expression. However, *in vivo* protein labeling analysis suggests that assembly of the ATP synthase  $\alpha$  and  $\beta$  subunits into the thylakoid membrane still occurs in *dpa1*. As a consequence of the destabilized ATP synthase complex, photophosphorylation is abolished even under reducing conditions. Further effects of the mutation include an increased light sensitivity of the plant and an altered photosystem II activity. At low light intensity, chlorophyll fluorescence induction kinetics is close to those found in wild type, but non-photochemical quenching strongly increases with increasing actinic light intensity resulting in steady state fluorescence levels of about 60% of the minimal dark fluorescence. Most fluorescence quenching relaxed within 3 min after dark incubation. Spectroscopic and biochemical studies have shown that a high proton gradient is responsible for most quenching. Thylakoids of illuminated *dpa1* plants were swollen due to an increased proton accumulation in the lumen. Expression profiling of 3292 nuclear genes encoding mainly chloroplast proteins demonstrates that most organelle functions are down-regulated. On the contrary, the mRNA expression of some photosynthesis genes is significantly up-regulated, probably to compensate for the defect in *dpa1*.

In oxygenic photosynthesis light-dependent electron transport from water to NADP<sup>+</sup> is coupled to synthesis of ATP (photophosphorylation) and energetically mediated by a transmembrane electrochemical proton gradient. Photophosphoryla-

tion, which essentially resembles oxidative phosphorylation, is carried out at the thylakoid membrane of photosynthetic eubacteria and chloroplasts and is catalyzed by a proton-translocating reversible ATPase ("ATP synthase"). The basic organization, structure, and composition of this protein complex have been extensively investigated on the eubacterial level as well as in mitochondria and plastids and were found to be vastly conserved (1, 2).

The plastid ATP synthase complex consists of nine different subunits, four of them are localized in the membrane integral CF<sub>0</sub> subcomplex ( $\alpha$ ,  $\beta$ ,  $\beta'$ , and  $c_{14}$ ) which is responsible for proton translocation, and five subunits constitute the extrinsic CF<sub>1</sub> subcomplex ( $\alpha_3$ ,  $\beta_3$ ,  $\gamma$ ,  $\delta$ , and  $\epsilon$ ) which forms the catalytic entity (3, 4). Three independent studies proved the rotation of the  $\gamma$  subunit relative to ( $\alpha\beta$ )<sub>3</sub> during ATP hydrolysis in the isolated F<sub>1</sub> (5–7) and recently in isolated F<sub>0</sub>F<sub>1</sub> complexes (8).

The  $\gamma$  subunit is responsible for the so-called "thiol modulation" or "redox modulation" due to two Cys residues able to form an intrapeptide disulfide bond (9). Upon reduction, the activation profile of ATP synthase is shifted toward lower proton gradients (10, 11). The seven amino acids Cys<sup>199</sup>–Cys<sup>205</sup> (numbering in *Arabidopsis*) are present only in land plants and green algae as in *Chlamydomonas reinhardtii* (10, 12). Nevertheless, differences in the redox regulation mechanism have been pointed out between algae and higher plants (13). Whereas in higher plants the re-oxidation of CF<sub>1</sub>, following a light-dark transition, takes over 1 h, in the alga *Dunaliella salina* CF<sub>1</sub> is several times faster re-oxidized by a specific endogenous oxidant (14). Only recently redox modulation of the  $\gamma$  rotation has also been reported (15).

In bacteria the genes for the two subcomplexes are organized in separate operons suggesting that the enzyme evolutionarily derived from a proton channel (F<sub>0</sub>) and an ATPase (F<sub>1</sub>) (16). The organization of the genes reflects also a possible mechanism of assembly. The bacterial F<sub>0</sub> and F<sub>1</sub> accumulate independently and associate then to the membrane to assemble a functional complex (17). However, only little is known about the assembly of the chloroplast enzyme (1). In *Chlamydomonas* neither CF<sub>0</sub> nor CF<sub>1</sub> is assembled, although the unpaired polypeptides are synthesized, if one of the nine subunits is missing. Several mutants in *Chlamydomonas* affected in different chloroplast-encoded subunits of the ATP synthase have been used to characterize the assembly process (18).

In *Arabidopsis* two genes, *atpC1* and *atpC2* (accession numbers M61741 and J05761, respectively), located on chromosomes 4 and 1, respectively, encode for the plastid  $\gamma$  subunit (19, 20). In plants grown under continuous illumination, *atpC1*

\* This work was supported by German Science Foundation Grant ME1794-2,1 (to J. M.). The costs of publication of this article were defrayed in part by the payment of page charges. This article must therefore be hereby marked "advertisement" in accordance with 18 U.S.C. Section 1734 solely to indicate this fact.

<sup>§</sup> The on-line version of this article (available at <http://www.jbc.org>) contains Sheet 1.

|| To whom correspondence should be addressed: Ludwig-Maximilians-Universität, Department Biologie I, Botanik, Menzingerstr. 67, 80638 München, Germany. Tel.: 49-89-17861288; Fax: 49-89-1782274; E-mail: meurer@botanik.biochemie.uni-muenchen.de.

is much higher expressed than *atpC2* (19). The two AtpC proteins in *Arabidopsis* share 73% sequence homology, whereas the homology of the AtpC subunits between other plants and AtpC1 in *Arabidopsis* is about  $88 \pm 4\%$ . This raises the intriguing question about the role(s) of the two *atpC* gene copies in *Arabidopsis*, and whether the two genes possess distinct functions and under which physiological conditions they become operative.

Proton efflux through the plastid ATP synthase, associated with ATP synthesis, results in an accelerated relaxation of the electric field-associated absorption change at 518 nm (21). This property has been used to identify coupling factor reduction mutants in *Arabidopsis* which grow poorly in dim light and showed slowed  $\Delta A_{518}$  decay after light-dark transition (22). One coupling factor quick recovery mutant, *cfq*, contains an E244D point mutation in the  $\gamma$  subunit leading to a decreased acidification of the lumen compared with wild type in the initial few minutes of the induction period under subsaturating light conditions. This mutant has been used to correlate non-photochemical chlorophyll fluorescence quenching (NPQ)<sup>1</sup> with  $\Delta pH$  (23).

In the present study we have identified the *Arabidopsis thaliana* mutant *dpa1* in which the *atpC1* gene has been inactivated by T-DNA insertion. The mutant has been characterized on the level of accumulation, activity, and assembly of ATP synthase. Deficiency of the  $\gamma$  subunit leads to loss of ATP synthesis and unusual NPQ which is much below the dark  $F_0$  level due to proton accumulation in the lumen. The pattern of mRNA expression of nuclear genes coding for chloroplast proteins in *dpa1* is interpreted as a compensatory effect.

#### EXPERIMENTAL PROCEDURES

**Plant Material, Growth Conditions, and Mutant Selection**—Seed sterilization and growth conditions of *dpa1* and wild type were as described (24) with the exception that only 1.4% (w/v) sucrose has been supplemented to the medium. Seedlings were grown under continuous light at a photon flux density of  $20 \mu\text{mol photons m}^{-2} \text{s}^{-1}$  and at a constant temperature of 21 °C if not otherwise indicated. Prior to illumination, plates were placed for 2 days at 4 °C to synchronize germination. Propagation of the *dpa1* mutant occurred via heterozygous offsprings. All comparisons between mutant and wild type were carried out with leaf material of the same developmental stage. Individual mutant plants of segregants grown in Petri dishes have been identified by chlorophyll (chl) fluorescence video imaging (FluorCam 690M; Photon Systems Instruments, Brno, Czech Republic). The FluorCam software package (protocol for quenching analysis) has been used to follow the chl fluorescence induction and to determine fluorescence parameters and PSII yield. The *dpa1* mutant could easily be distinguished from wild type plants due to a strong NPQ (see below).

**Molecular Mapping and Complementation Studies**— $F_1$  populations were produced by pollinating emasculated flowers of the accession Landsberg erecta with Wassilewskija plants heterozygous for the *dpa1* mutation.  $F_2$  families selected for the mutant offsprings were grown on medium, and individual mutant plants were chosen for genetic mapping of the mutation with molecular markers. The oligonucleotides 5'-CAGTCGAATCTTGATGACCGTCGATGATG-3' and 5'-GTTTCGTCGAGAATCAGAGTGGCTC-3' were used as a simple sequence length polymorphism marker Cer452226 (25) located 850 kb upstream of the *atpC1* gene on the bacterial artificial chromosome F4C21. This marker is polymorphic between Landsberg and Wassilewskija producing 203- and 285-bp PCR products, respectively.

The full-length coding sequence of the intron-less *atpC1* gene was amplified by *Pfu* polymerase from wild type genomic DNA using the forward primer 5'-AACAAAAAATGGCTTGCTCTAATCTAAC-3' and the reverse primer 5'-AAGAGGGTCTAGACAAATCAAACCTGT-

GC-3', which inserts an XbaI restriction site at the 3'-end of the gene. The XbaI-digested and -purified PCR product was ligated into the SmaI/XbaI sites of the binary vector pS001-VS under control of the cauliflower mosaic virus 35S rRNA promoter (26). Successful cloning was verified by sequencing. The construct was introduced into progenies of plants that segregate the mutation via *Agrobacterium* using the floral dip method (27). Transformant plants were efficiently selected on rock wool (Grodan, Hobro, Denmark) immersed in 10 mg/liter sulfadiazine prior to spreading the seeds (28).

For PCR analysis of transformed lines (see Fig. 1) the following primers have been used: Atactr (5'-GCTCATTCTGTGCGGATTCAGG-3') and Atactf (5'-TCCTAGTATTGTGGGTCGCTCTCG-3') of the *actin3* gene as a control; primer 1 (5'-CGAACCTCCACTAATACCCAGCC-3') of the *atpC1* promoter; primer 2 (5'-CGTCTCTTCGTGAGCTCAGAGACCGTATCG-3') of the 5' *atpC1* coding region; primer 3 (5'-GCATAGATGCACTCGAAATCAGCC-3') of the left border of the T-DNA; primer 4 (5'-GGTGATAAAGCGAGTACGGTGTGATCAGC-3') of the 3' *atpC1* coding region; and primer Pv (5'-GCCATCGTTGAAGATGCTCTGCCG-3') of the 35S promoter.

**Northern and Southern Analyses**—Total RNA and DNA were isolated and subjected to Northern and Southern analysis, respectively, as described (24, 29–31). Hybridizations with <sup>32</sup>P-labeled probes were carried out for 1 h at 68 °C in Rapid Hybridization Buffer (Amersham Biosciences). The signals were analyzed on autoradiographs using Fuji Bio Imaging plates type BASIII, a Fuji Bio Imaging analyzer, and the Aida software package (Raytest, Sprockhövel/Germany). Probes for *atpH1*, *atpF*, *atpA*, and *atpC1* used for Northern analysis were as described (32). To confirm the array expression data, probes for *petC*, *psbS*, *lhcB6*, and *psaD1* genes were used in Northern analysis. The full-length cDNAs obtained from the ABRC (*Arabidopsis* Biological Resource Center at Ohio State) were amplified using the vectorial (pZLI, Invitrogen) forward primer 5'-TAATACGACTCACTATAGGG-3' and the reverse primer 5'-ATTTAGGTGACACTATAG-3'.

**Real Time PCR Technique**—The LightCycler Thermal Cycler System (Roche Applied Science) was used to perform quantitative two-step reverse transcriptase-PCR for *atpC1*, *atpC2* mRNA, and 18S rRNA applying the SYBR Green protocol (33). cDNA synthesis was carried out with total RNA using SuperScript II RNase H<sup>-</sup> Reverse Transcriptase (Invitrogen) and hexanucleotides according to the manufacturer's instructions (Roche Applied Science). Primer combinations specific for the 5'-ends of *atpC1* (primer 2 and 5'-GGTTAAGGGAACATCGACATCATCGG-3'), *atpC2* (5'-GCTTCGAGCTCAGAGTCTACTCTT-3' and 5'-C-CAGTAACAACAACCAAGCAACTCTC-3'), and the 18S rRNA (5'-GCTCAAAGCAAGCCTACGCTCTGG-3' and 5'-GGACGGTATCTGATC-GTCTTCGAGCC-3') were chosen. After addition of MgCl<sub>2</sub> (4 mM) and template cDNA to the master mix, an initial denaturation step followed by 45 cycles of denaturation (95 °C for 15 s), annealing (58 °C, *atpC1* and *atpC2*, or 63 °C, 18S rRNA for 5 s) and extension (72 °C for 1 s/20 bp) were performed. All ramp rates were set to 20 °C per s. Serially diluted samples of *Arabidopsis* genomic DNA, corresponding to 15 ng to 1.5 pg, were used for calibration. Specific amplification has been confirmed by melting curve analysis and agarose gel electrophoresis.

**Photophosphorylation**—Chloroplast thylakoids from *Arabidopsis* leaves were prepared as described for spinach (34). The reactions were conducted in a  $\Delta pH$  clamp instrument as described (35). The reaction cell of 2.5-ml volume contained a medium consisting of 25 mM Tricine buffer, pH 8.0, 5 mM dithiothreitol, 5 mM MgCl<sub>2</sub>, 5 mM <sup>32</sup>P-labeled Na<sub>2</sub>HPO<sub>4</sub>, 50 mM KCl, 50  $\mu\text{M}$  phenazine methosulfate, and thylakoids corresponding to a chl concentration of 25  $\mu\text{g/ml}$ . The experiments were conducted at pre-chosen  $\Delta pH$  values (35, 36) which were kept constant throughout the experiment by the employed clamp device.  $\Delta pH$  was continuously controlled by the fluorescence quenching of 9-aminoacridine. The fluorescence signal was calibrated as described (37).

The thylakoids were pre-illuminated for 2 min to obtain the pre-chosen proton gradient. Then 0.5 mM ADP was added in the light. After 10, 20, and 30 s, 0.2-ml samples were taken and deproteinized by HClO<sub>4</sub> (final concentration 0.6 M). The formed <sup>32</sup>P-labeled organic phosphate was determined as described (38).

**Immunological and Translation Analyses**—Thylakoid membrane proteins of 3-week-old plants were isolated as described (39). Proteins were quantified (40), and samples were heated for 5 min at 80 °C in 2% SDS mixed with 1/10 volume of glycerol/dye solution and immediately applied onto SDS-PAGE at 30 mA for 12–15 h at room temperature. The protein pattern was visualized in silver-stained gels (41). For immunodetection, proteins were transferred to PVDF membranes (Pall Biodyne, Dreieich, Germany) by semi-dry electroblotting (Peqlab, Erlangen, Germany). The membranes were incubated with antisera raised against thylakoid membrane proteins, and signals were identi-

<sup>1</sup> The abbreviations used are: NPQ, non-photochemical quenching; chl, chlorophyll; PAM, pulse amplitude modulation; PSI and PSII, photosystem I and II, respectively; Q<sub>A</sub>, primary electron acceptor quinones of PSII; qE, high energy quenching; WT, wild type; PVDF, polyvinylidene difluoride; T-DNA, transfer DNA; Tricine, N-[2-hydroxy-1,1-bis(hydroxymethyl)ethyl]glycine.

fied by the enhanced chemiluminescence technique (Amersham Biosciences). Most of the antibodies used in this study were raised in rabbits against *Chlamydomonas* or spinach polypeptides (24). For *in vivo* labeling analysis intact leaves of 3-week-old plants were immersed in a  $\frac{1}{2} \times$  MS solution containing 50  $\mu$ Ci of [ $^{35}$ S]methionine for 20 min (42). Subsequently, thylakoid membrane proteins were isolated, subjected to SDS gel electrophoreses, and transferred to PVDF membranes. Incorporation was detected by fluorography (43).

**Electron Microscopy**—Sample preparations for ultrastructural analysis and electron microscopy were performed as described (44).

**Fluorometric and Absorption Studies**—chl *a* fluorescence measurements were performed with 3-week-old plants using a commercial pulse amplitude modulated fluorometer PAM 101 interfaced with the PAM data acquisition system PDA-100 (Walz, Effeltrich, Germany). The fiber optic was held 2 mm distant from the upper side of plants grown under sterile conditions in Petri dishes. Leaves were dark-adapted for 5 min prior to the induction fluorescence measurements. The minimal ( $F_o$ ), steady state ( $F_s$ ), and maximal ( $F_m$ ) fluorescence yield, and the variable fluorescence ( $F_v$ ), calculated as ( $F_m - F_o$ ), as well as the ratio  $F_v/F_m$ , which reflects the potential yield of the photochemical reaction of PSII (45), were recorded at 20 °C, unless noted otherwise. Photochemical quenching and NPQ was determined as described (46). The intensity of the saturating light flash (800 ms) used for detection of  $F_m$  and the maximal fluorescence during induction,  $F_m'$ , was 4000  $\mu$ mol photons  $m^{-2} s^{-1}$ . For nigericin studies, leaves of 3-week-old plants were harvested and cut into small pieces with a sharp razor blade at 4 °C in 50 mM HEPES (pH 7.6), 330 mM sorbitol, 1 mM  $MgCl_2$ , 1 mM  $MnCl_2$ , 2 mM EDTA, and 0.2% (w/v) defatted bovine serum albumin. The resuspension buffer was supplied with 0.1 mM methylviologen as an electron acceptor in all samples and, when indicated, with 2  $\mu$ M nigericin as an ionophore (47).

**Expression Profiling Using Nuclear Arrays**—The 3292 gene sequence tags array representing genes known or predicted to code for proteins having a chloroplast transit peptide has been described previously (48, 49). At least three experiments with different filters and independent cDNA probes derived from plant material corresponding to pools of at least 50 individuals were performed for each condition or genotype tested, thus minimizing variations between individual plants, filters, or probes. cDNA probes were synthesized by using a mixture of oligonucleotides matching the 3292 genes in antisense orientation as primer, and hybridized to the gene sequence tags array as described previously (48, 49). Images were read using the Storm PhosphorImager (Amersham Biosciences). Hybridization images were imported into the *ArrayVision* program (version 6; Imaging Research Inc., Ontario, Canada) and statistically evaluated (Bonferroni-adjusted significance test corresponding to a confidence interval of 0.9999), using the *ArrayStat* program (version 1.0 Rev. 2.0; Imaging Research). Normalization of data was performed with reference to all spots on the array as described previously (48, 49).

**Miscellaneous**—Basic molecular biology methods were performed as described (31). Nucleotide sequences were determined by the dideoxy chain termination method (50). Energy transfer fluorochrome dideoxynucleotide labeling (51) was used for detection of sequencing products using the ABI 377 system (Applied Biosystems).

## RESULTS

**Identification and Phenotype of the *Dpa1* Mutant**—The F2 progeny of 1100 EMS-treated seeds and 75 preselected pale mutants from T-DNA collections (53) obtained from the *Arabidopsis* Biological Resource Centre (Ohio State University, Columbus, OH) have been used for screening. 87 mutant plants were selected by their non-photoautotrophic growth on soil. They developed pale green cotyledons but no primary leaves. Cultivation on sucrose-supplemented MS medium (52) often rescued the mutant seedlings, leading to a nearly normal pigmentation and development. Under these conditions the mutants could often hardly be distinguished from wild type plants, although growth rates were slightly retarded. Seven plants showing a high dark level of fluorescence ( $F_o$ ) but a lower level during induction were selected from the collection by imaging analysis (Fig. 1A). In six plants the lowest fluorescence level became apparent after about 1–2 min, and the fluorescence again slowly increased close to the  $F_o$  level during induction. This unusual fluorescence behavior we have already observed

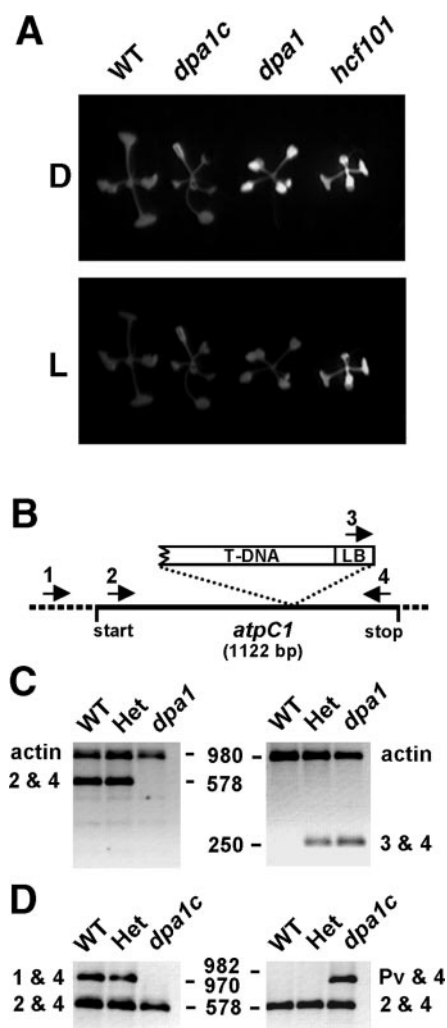


**FIG. 1. Mutant screen, T-DNA insertion, and complementation studies.** A, chl fluorescence of seedling lethal mutants was initially recorded by fluorescence imaging. The *dpa1* mutant has been selected due to its high dark fluorescence level,  $F_o$  (D), and its normal steady state fluorescence level ( $F_s$ ) during illumination (L). Photosynthetic electron transport mutants (*hcf101*) showed a high fluorescence level under both conditions, whereas complemented homozygous mutant plants (*dpa1c*) behaved like wild type. B, schematic presentation of the insertion of the truncated T-DNA into the *atpC1* gene and of the primers used for the PCR analysis. *Primer 1* was chosen from the *atpC1* promoter, *primers 2* and *4* from the *atpC1* coding region, and *primer 3* from the left border of the T-DNA. C, PCR analysis of wild type (WT), heterozygous lines (*Het*), and mutant plants. The data demonstrate homozygosity of *dpa1* because primers 2 and 4 did not amplify, whereas the internal control reaction using primers of the *actin3* gene was positive in *dpa1*. The PCR product using primers 3 and 4 demonstrates the insertion and the orientation of the T-DNA. D, analysis of complemented *dpa1c* plants. Primers 1 and 4 did not amplify in the complemented line due to the insertion of the T-DNA into the coding region of the endogenous gene. Successful complementation is proven by amplification with primers 2 and 4 of *atpC1* as well as primers 4 and *Pv* (chosen from the 35S RNA promoter of the binary vector).

previously in several *high chlorophyll fluorescence (hcf)* mutant plants (24).

In one mutant, *dpa1*, light-dependent quenching of  $F_o$  was stable during induction. Therefore, we have chosen *dpa1* for the present study.

This increased NPQ was indicative of photosynthetic electron transport activity in *dpa1* in contrast to a high chlorophyll fluorescence phenotype of photosystem I mutants such as *hcf101* (Fig. 1A) (24). The screened seedling lethal *dpa1* mutant of *A. thaliana*, accession Wassilewskija, originated from the T-DNA insertion collection.

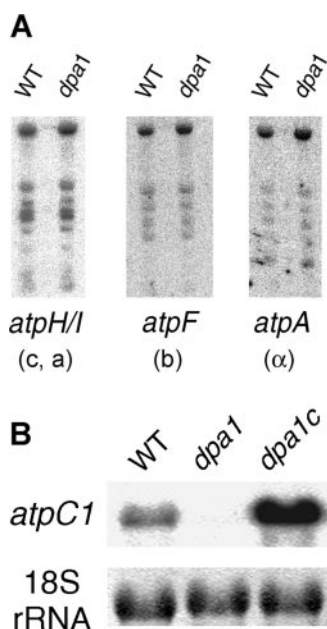


**FIG. 2. Northern analysis of plastid and nuclear genes.** Expression analysis of plastid genes encoding ATP synthase subunits (A) and the nuclear *atpC1* and *18S* rDNA genes (B). Total RNA from 3-week-old mutant and wild type plants was analyzed by Northern hybridization. As probes PCR-amplified products of the genes *atpH/I*, *atpF*, *atpA*, and *atpC1* were used. A, 5  $\mu$ g of RNA were loaded. B, 5  $\mu$ g RNA have been loaded to confirm inactivation of *atpC1* in *dpa1* and to estimate *atpC1* expression in *dpa1c* complemented lines.

**Inactivation of the *atpC1* Gene**—Initially, we have tried to isolate flanking genomic regions of the right border of the T-DNA by inverse PCR. Each attempt to get a specific product failed. We backcrossed the mutation in order to confirm the Mendelian segregation of *dpa1*, to remove possible background mutations and to generate a mapping population. The *dpa1* mutation was mapped to the upper part of chromosome 4 by the use of the molecular Cer452226 marker closely located to *atpC1* (see “Experimental Procedures”). Forty-eight meiotic chromosomes of individual F2 mutant plants derived from backcrosses to the accession Landsberg have been used in this study. No recombinations have been identified, indicating that the *dpa1* mutation is closely linked to the *atpC1* gene.

Southern analyses with genomic DNA from *dpa1*, wild type, and heterozygous plants using probes of the T-DNA left border and the *atpC1* gene resulted in restriction fragment length polymorphisms showing that there is a T-DNA insertion in the region of *atpC1* (data not shown).

Due to the close location of the mutation to *atpC1* and the observed restriction fragment length polymorphism, primers of the *atpC1* gene and of the T-DNA borders were chosen in order to identify the site of T-DNA insertion. Only primers of the left border together with gene-specific primers were able to amplify indicating that the right border was truncated (Fig. 1, B and C). By sequencing PCR products obtained with primers 3 and 4, the exact location of the T-DNA at position +603 bp relative to the start codon of the *atpC1* gene could be defined (Fig. 1, B and C). With primers 2 and 4, *atpC1* could not be amplified in the mutant, but the expected product of 578 bp was generated in wild type and heterozygous plants (Fig. 1C). The PCRs also included the two primers of the *actin3* gene as an internal control that amplified in both wild type and mutant plants (Fig. 1C).

Northern analyses of transcripts of plastid genes encoding subunits of the chloroplast ATP synthase, *i.e.* *atpA*, *atpH/I*, and *atpF*, showed that their expression was not altered in the

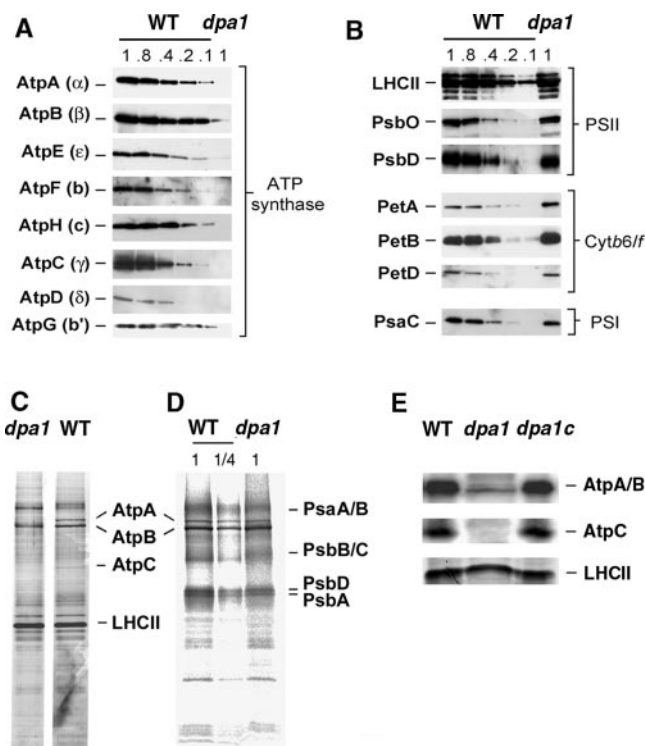


**FIG. 3. Levels and translation of thylakoid membrane proteins.** Immunoblot analysis of ATP synthase subunits (A) and other photosynthetic membrane complexes in wild type and *dpa1* (B). Size-fractionated membrane proteins were immunodetected with antisera raised against individual subunits of the four major thylakoid membrane complexes as indicated. 10, 8, 4, 2, and 1  $\mu$ g of membrane proteins of wild type and 10  $\mu$ g of proteins of *dpa1* were loaded. 1 corresponds to 10  $\mu$ g of protein. C, silver staining; D, *in vivo* labeling of thylakoid membrane proteins. Incorporation of [ $^{35}$ S]methionine occurred in the presence of cycloheximide. Thylakoid membrane proteins of wild type and mutants with equivalent amounts of radioactivity (100,000 cpm (lanes WT and *dpa1*) or 25,000 cpm (lane WT 1/4)) were separated by electrophoresis, transferred onto PVDF membranes, and analyzed by fluorography. E, immunoblot analysis of wild type, *dpa1* and complemented mutant lines, *dpa1c*. Three-week-old plants were used for all analyses.

mutant (Fig. 2A). On the contrary, *atpC1* was not expressed in *dpa1* (Fig. 2B). Real time reverse transcriptase-PCR analysis has shown that *atpC2* is  $209 \pm 35$  times lower expressed than *atpC1* in wild type leaves and that the expression of *atpC2* is unaltered in *dpa1* as compared with the wild type.

**The *atpC1* Gene Complements the *dpa1* Mutation**—In order to confirm that the phenotype of the *dpa1* mutant is indeed caused solely by the insertional inactivation of the *atpC1* gene, complementation studies were performed. Mutant plants expressing the wild type *atpC1* gene under control of the 35S RNA cauliflower mosaic virus promoter were selected in the progeny of transformed plants heterozygous for the mutation (Fig. 1D). Northern analysis of complemented lines confirmed that *atpC1* is significantly overexpressed as compared with wild type plants (Fig. 2B).

Homozygous *dpa1* transformants were able to grow photoautotrophically, exhibited normal growth rates, and were green in appearance. The chl fluorescence parameters  $F_v/F_m$  (0.8) as well as photochemical quenching (0.85) and NPQ (0.18) of complemented lines were within the standard deviations of the wild type (see below).

**Accumulation of the Plastid ATP Synthase Is Abolished in *dpa1***—The accumulation of the ATP synthase and other complexes of thylakoid membranes of *dpa1* and wild type was compared by using a collection of antisera raised against eight individual ATP synthase polypeptides and, as a control, repre-

TABLE I  
ATP production in isolated chloroplasts at different  $\Delta pH$  and redox conditions

$\Delta pH$	WT		dpa1	
	Oxidized	Reduced	Oxidized	Reduced
	$\mu\text{molATP/mgChl}\cdot\text{h}$			
2.4	15	15	2.7	6.6
2.5	31.7	64	1.9	6.2
2.8	73.1	116.5	1.9	5.4
2.9	89.3	140	2.6	6.8

sentative polypeptides of PSI, PSII, and the cytochrome  $b_{6/f}$  complex (24). All nuclear and plastid-encoded subunits of the ATP synthase analyzed failed to accumulate in significant amounts in *dpa1* (Fig. 3A). The dilution series of wild type membranes demonstrated that levels of ATP synthase subunits were reduced to less than 5%. Amounts of several subunits such as AtpA, AtpC, AtpH, AtpD, and AtpG were below the limit of detection. Only little differences in steady state levels were observed for other nuclear and plastome-encoded proteins of PSII, e.g. LHCII, PsbO, PsbD (D2), PSI, and PsaC, analyzed in *dpa1* (Fig. 3B). In contrast, levels of proteins of the cytochrome  $b_{6/f}$  complex, e.g. PetA and PetB, were increased in *dpa1*.

Some ATP synthase complexes might assemble in the mutant, which contain the *atpC2* gene product. However, expression of *atpC2* is not sufficient to allow photoautotrophic growth, detection of the  $\gamma$  subunit, and significant accumulation of any other subunit that belongs to the ATP synthase. Taken together, immunoblot analyses indicate that loss of the ATP synthase constitutes the primary defect in *dpa1*.

Although *atpC1* is overexpressed in complemented lines (Fig. 2B), the Western data show that neither the  $\gamma$  subunit nor the ATP synthase accumulate to higher levels as compared with the wild type (Fig. 3E).

**Decreased Stability of the Plastid ATP Synthase Subunits**—In silver-stained gels it was already visible that the two large  $\alpha$  and  $\beta$  subunits of the ATP synthase and the  $\gamma$  subunit were depleted in *dpa1* (Fig. 3C), although amounts and patterns of all the other thylakoid membrane proteins were comparable with those of the wild type. A diffuse band, the identity of which is presently unknown, comigrates with the AtpB protein in the gels. The rate of synthesis of plastid-encoded ATP synthase proteins was investigated by pulse-labeling experiments with [ $^{35}\text{S}$ ]methionine (Fig. 3D). To reduce the complexity of labeling, synthesis of the nuclear encoded chloroplast proteins was blocked with cycloheximide so that only plastome-encoded proteins appeared. Labeled proteins were purified and subjected to SDS-gel electrophoreses. The appearing signals in the gels could be assigned to individual subunits of the thylakoid membrane, i.e. PsaA/B, AtpA/B, PsbB/C, and PsbA/D, due to their abundance and known electrophoretic mobilities and by mutant analysis (32). The protein labeling patterns in the mutant and wild type were identical with respect to the size and the numbers of all detectable polypeptides and their intensity of labeling. The PSII subunits PsbA, PsbB, PsbC, and PsbD, and the ATP synthase  $\alpha$  (AtpA) and  $\beta$  (AtpB) subunits were synthesized at about normal rates in the mutant, whereas steady state levels of the  $\alpha$  and  $\beta$  subunits were reduced by more than 95% as compared with the wild type (Fig. 3A). Therefore, lack of the ATP synthase subunits in *dpa1* is caused by a decreased stability of all subunits that constitute the complex in the mutant background. However, the fact that the ATP synthase  $\alpha$  and  $\beta$  subunits are synthesized at normal levels and are found in the membrane fraction implies that, interestingly, accumulation and incorporation of both subunits into the thylakoid membrane is independent of the  $\gamma$  subunit.

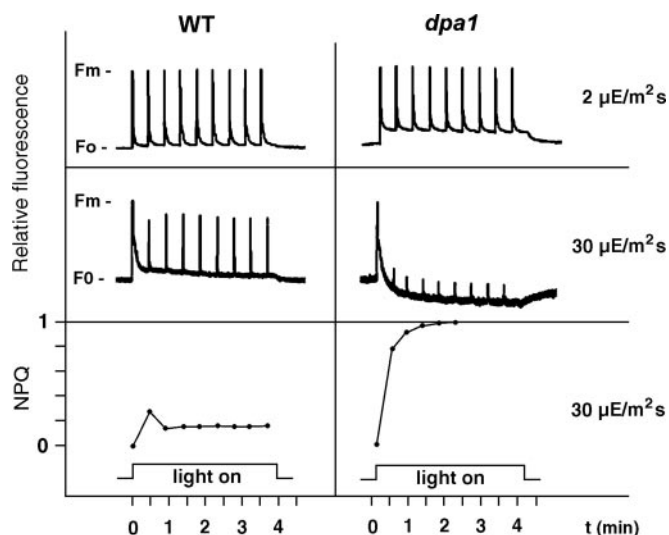


FIG. 4. *In vivo* chlorophyll fluorescence induction and NPQ analysis in *dpa1*. Actinic light has been applied at time 0 together with a saturating pulse to dark-adapted plants in order to record the maximal fluorescence. Consecutive pulses have been applied at intervals of 30 s. The actinic light intensity was  $2 \mu\text{mol of photons m}^{-2} \text{s}^{-1}$  and  $30 \mu\text{mol of photons m}^{-2} \text{s}^{-1}$ .

**The Activity of the Plastid ATP Synthase Is Abolished in *dpa1***—The immunological data have been supported by analysis of ATP production with isolated thylakoids (Table I). The rate of photophosphorylation depended on the magnitude of  $\Delta pH$  applied and attained  $112.1 \mu\text{mol of ATP mg of chl}^{-1} \text{h}^{-1}$  at  $\Delta pH$  3.0 in wild type thylakoids. As reported for spinach chloroplasts, the ATP synthesis rate was increased in an intermediate  $\Delta pH$  range from 2.5 to 3.0 under reducing conditions, indicating a lower  $\Delta pH$  profile for activation of the ATP synthase (12). In mutant thylakoids, on the other hand, phosphorylation activity was low and  $\Delta pH$ -independent both under oxidized and reduced conditions, i.e. probably unrelated to photophosphorylation.

**Inactivation of PSII Depends on Light Intensity in *dpa1***—Deficient ATP synthases in *Chlamydomonas* are known to affect PSII stability which involves ClpP, a chloroplast-encoded peptidase (54). Therefore the functional state of PSII has been monitored by non-invasive chl fluorescence measurements (45). Analysis of *dpa1* mutant seedlings revealed a decrease in  $F_s/F_m$  ( $0.60 \pm 0.05$  versus  $0.80 \pm 0.02$  in the wild type) which is indicative of a partially impaired PSII. Light intensities of  $2 \mu\text{mol photons m}^{-2} \text{s}^{-1}$  for fluorescence induction did not significantly increase the  $F_s$  above the  $F_o$  level in wild type plants, and saturating light pulses were able to completely induce the  $F_m$  level during induction (Fig. 4). In *dpa1* low light significantly increased the  $F_s$  to 20% of  $F_o$ , indicating that electrons are not efficiently released from PSII and probably keep the primary quinone acceptor of PSII,  $Q_A$ , partially reduced.  $F_m$  could be reached during induction indicating that no significant proton accumulation or NPQ takes place at this low light intensity in *dpa1*. Light-induced quenching of chl fluorescence severely depended on the chosen light intensity. Under low light of  $2 \mu\text{mol of photons m}^{-2} \text{s}^{-1}$  NPQ was close to zero in both wild type and *dpa1*; under still moderate light intensities of  $30 \mu\text{mol of photons m}^{-2} \text{s}^{-1}$  a very strong NPQ was observed in *dpa1* reaching values of 1 after 2 min of induction, while in wild type NPQ was below 0.2 (Fig. 4). Depending on the light intensity the fluorescence dropped far below the dark  $F_o$  level which could be quenched up to 40%. This high non-photochemical quenching mechanism did not allow light pulse-dependent increase of the fluorescence above the  $F_o$  level after 2 min of induction (Fig. 4).

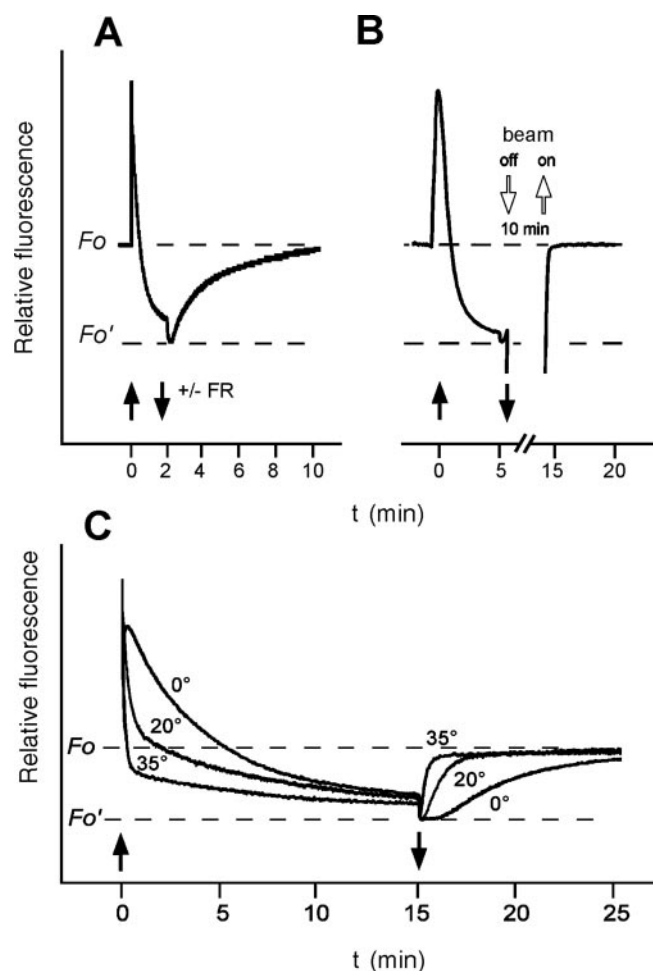


FIG. 5. Analysis of the post-illumination fluorescence increase in *dpa1*. A, the actinic light intensity given for 2 min was  $50 \mu\text{mol photons m}^{-2} \text{s}^{-1}$ . Induction and darkening is indicated by filled upward and downward arrows, respectively. The relaxation rate of fluorescence quenching was identical with or without far-red background light (intensity 8 of the PAM settings) after switching off actinic light. B, after 5 min of fluorescence induction, the actinic light and the measuring beam (open arrows) were switched off. Ten minutes later the beam was switched on again, and the  $F_o$  value was immediately recovered. C, light-induced fluorescence quenching at  $30 \mu\text{mol photons m}^{-2} \text{s}^{-1}$  and the dark relaxation after 15 min of induction has been recorded at 0, 20, and 35 °C. The curves were normalized to the  $F_o'$  level (lowest  $F_o$  value immediately after switching off the light).

The quenching below  $F_o$  was reversible and relaxed to about 90% within 3 min dark incubation; complete relaxation took about 10 min (Fig. 5). It was investigated whether the post-illumination increase of the fluorescence in *dpa1* was mainly due to high energy quenching (qE), which is known to depend on the luminal proton concentration (55). Far-red light, which selectively excites PSI, has been applied after induction but was unable to change the relaxation rate, independently of which intensity has been used (Fig. 5A). Therefore, the fluorescence increase in the dark after switching off actinic light could not be caused by reduction of quinones in *dpa1*.

In order to exclude the possibility that the weak measuring beam (setting of the PAM beam intensity was 3 and 4), which is permanently on during measurements in the dark, was responsible for the dark increase of the fluorescence in *dpa1*, both the measuring beam and the actinic light were switched off for 10 min after induction (Fig. 5B). At this time the dark level could be reached again within a few seconds when applying the measuring beam confirming that the fluorescence increase is independent of reduction of  $Q_A$  by the weak measuring beam.

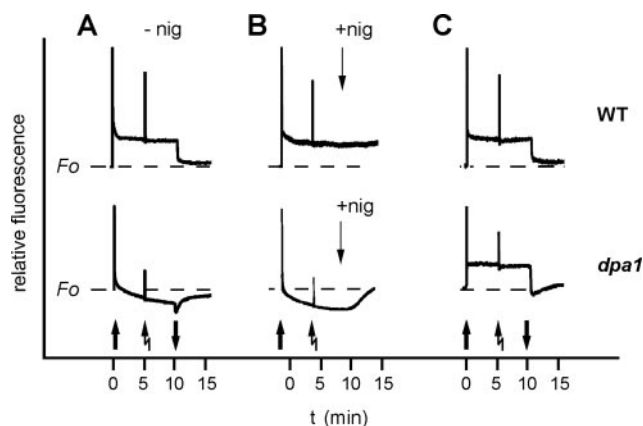


FIG. 6. Effect of nigericin on fluorescence traces. A, the actinic light intensity was  $30 \mu\text{mol photons m}^{-2} \text{s}^{-1}$ . Chlorophyll fluorescence of *dpa1* and wild type leaves cut in small pieces has been recorded. The fluorescence behavior was close to intact leaves in both mutant and wild type. The continuous actinic light was switched on (upward arrow) followed by a saturating pulse 5 min later (zigzag arrow). Ten minutes later the actinic light was either switched off (downward arrow; A and C) or B,  $2 \mu\text{M}$  of the uncoupler nigericin (*nig*) was supplied. C, nigericin was added 10 min before fluorescence analysis.

Therefore, we suppose that the fluorescence increase in the dark is reflected by relaxation of the high energization of the thylakoid membrane. This assumption is consistent with the finding that the fluorescence increase was severely slowed down at a lower temperature when the thylakoid membrane is less leaky for protons (Fig. 5C). Lowering the temperature to 0 °C decreased the relaxation rate considerably, and increasing the temperature to 35 °C increased the relaxation rate. In addition, the kinetics of fluorescence quenching is also temperature-sensitive (Fig. 5C). Increasing the temperature to 35 °C accelerated the quenching process, and decreasing the temperature to 0 °C slowed down the kinetics. However, the steady state fluorescence level below  $F_o$  was nearly identical at 0, 20, and 35 °C after 15 min. This might well be explained by the temperature dependence of the xanthophyll cycle.

To investigate further the quenching mechanism, fluorescence induction curves were analyzed in the presence of the ionophore nigericin (Fig. 6). If quenching in *dpa1* was due to accumulating protons in the lumen, the action of the uncoupler should prevent this tendency. Indeed, when nigericin was applied during induction, quenching of  $F_o$  started to relax in *dpa1* and fluorescence again reached levels above  $F_o$  (Fig. 6B). When nigericin was supplied 10 min before starting the fluorescence measurement, *dpa1* failed to perform strong NPQ, and the fluorescence traces were close to that found in wild type. Quenching of  $F_o$  in the darkness immediately after switching off actinic light was almost negligible (Fig. 6C).

**Ultrastructure of *dpa1* Chloroplasts**—Electron micrographs of leaves from illuminated 3-week-old plants revealed an impaired structure of the chloroplast (Fig. 7). The mutant formed grana stacks which were disordered and not strictly orientated in parallel to each other probably because they were not always interconnected by stroma thylakoid membranes. The luminal space was swollen indicative of a light-dependent high proton gradient across the thylakoid membrane which leads to influx of osmotically active ions (54). The thylakoid membrane system was not reduced in *dpa1*, but mutant chloroplasts were deficient of any starch grains.

**Expression of mRNAs for Nucleus-encoded Chloroplast Proteins in *dpa1***—To investigate further effects of the *atpC1* mutation, the expression levels of nuclear genes that contribute to chloroplast functions were determined by DNA array analysis. This was carried out on a set of 3292 gene sequence tags, about

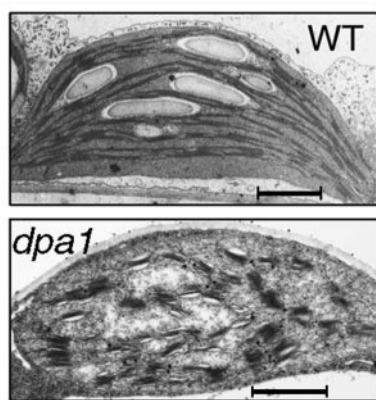


FIG. 7. Ultrastructure of chloroplasts from 3-week-old wild type and *dpa1* leaves. Both wild type and mutant plants were grown on sucrose-supplemented medium and illuminated prior to leaf fixation. Plants of the same age were selected for electron microscopic analyses. Bar, 1  $\mu$ m.

81% of which code for chloroplast-targeted proteins, and their expression patterns in *dpa1* mutants were compared with those in wild type (48, 49). Differential gene expression values (*dpa1* versus wild type) were determined by comparing hybridization signals. Statistical analysis of the expression data revealed that 1930 genes showed significant differential expression in *dpa1*. An unbalanced response of the nuclear chloroplast transcriptome was observed in the mutant, with the vast majority of differentially expressed genes being down-regulated (1765 genes down- and 165 genes up-regulated).

The differentially expressed genes in *dpa1* were grouped into 13 major functional categories, including photosynthesis (dark or light reaction), primary and secondary metabolism, transcription, protein synthesis, transport, and others (Fig. 8) (Supplemental Material). Most of the different functional gene classes followed the general trend of down-regulation. However, genes for the light and dark phase of photosynthesis were up-regulated more than others. Closer inspection of photosynthetic gene expression uncovered that in particular genes coding for proteins of the ATP synthase, the cytochrome *b6/f* complex, PSI, or the Calvin cycle were up-regulated in *dpa1* (Table II), whereas differentially expressed genes coding for PSII tended to be up- and down-regulated. Because the analysis of the expression of photosynthetic proteins (Fig. 3) and of chlorophyll fluorescence characteristics implied that photosynthetic electron flow still occurs in the *dpa1* mutant, the mRNA expression changes might indicate that the plant is able to monitor the altered photosynthetic state of the chloroplast (e.g. the increased lumen acidification) and reacts by regulating appropriate photosynthetic genes. For example, from the analysis of steady state levels of photosynthetic proteins, it appears that the level of PSI-C is decreased in the mutant (Fig. 3B) and the up-regulation of other PSI genes could be a compensatory reaction of the plant to prevent an even higher reduction of this photosystem. In the same way expression of the two remaining nuclear genes of the ATP synthase, *atpD* and *atpG*, is increased in *dpa1* (Table II).

#### DISCUSSION

*The  $\gamma$  Subunit Is Essential for Assembly of the Plastid ATP Synthase*—In the present study we characterized the *dpa1* mutation in *Arabidopsis* which has been induced by T-DNA insertion into the *atpC1* gene encoding the  $\gamma$  subunit of the chloroplast ATP synthase. The low endogenous expression of *atpC2* is not altered in *dpa1* and does not result in detectable amounts of the  $\gamma$  subunit in the mutant (Fig. 2B). *AtpC2* contains the unique domain, not present in mitochondrial and

bacterial  $\gamma$  subunits, which is known to be responsible for redox regulation of the enzyme (56, 57). Due to the low homology between *AtpC1* and *AtpC2* it is conceivable that the two subunits have been maintained for adjustment under changing environmental or tissue-specific conditions or in order to keep the plastid ATP synthase under proper photosynthetic control. The two *atpC* genes are not conserved in the amino-terminal part of the transit peptide and are not found in duplicated genomic blocks assuming two independent gene transfers to the nucleus (58, 59).

Overexpression of *atpC1* is not sufficient to increase amounts of the ATP synthase complex in complemented lines (Fig. 3C). Thus, an increased expression of several or all genes of the ATP synthase might be necessary to regulate the abundance of the complex or, more likely, that regulation of complex abundance takes place on a translational or post-translational level (18). Biogenesis of ATP synthases in eubacteria and mitochondria proceeds through assembly of the soluble  $F_1$  followed by association to the transmembrane  $F_0$  subcomplex (17, 60). The independence of assembly of the two subcomplexes is abolished in plastids of the green algae *Chlamydomonas* where a concerted assembly of  $CF_1$  and  $CF_0$  subunits has been reported for mutants affected in different subunits (61–63). The same holds true for *dpa1*, where lack of the nuclear encoded  $\gamma$  subunit affects the accumulation of all other nuclear and plastid-encoded subunits that constitute the ATP synthase. A model for the assembly pathway that resulted from different mutant analyses and reconstitution experiments predicts an early stage formation of  $\alpha\beta$  heterodimers followed by trimerization upon interaction with the  $\gamma$  subunit (18). *In vivo* labeling studies have shown that the plastid-encoded  $\alpha$  and  $\beta$  proteins of the  $CF_1$  subcomplex of 55.4 and 53.8 kDa, respectively, are translated at normal rates (Fig. 3D). Surprisingly, *de novo* synthesized  $\alpha$  and  $\beta$  subunits are associated with the membrane even in the absence of the  $\gamma$  subunit in *dpa1*. This provides new insights into the assembly pathway of the plastid ATP synthase and may imply that either  $\gamma$  is not necessary for the formation of the  $\alpha\beta$  hexamers prior to assembling into the membrane or that the  $\alpha\beta$  dimer can already associate to the membrane mediated by yet unidentified chaperones in the chloroplast. In yeast mitochondria at least two chaperones play an important role in the assembly of the  $\alpha$  and  $\beta$  subunits into the  $F_1$  oligomer (64). Nevertheless, binding of  $\alpha$  and  $\beta$  to  $CF_0$  mediated by  $\delta$  and  $b'$  cannot be excluded. The *dpa1* mutant now provides a starting material to investigate the function of *atpC2*, recombinant forms of the  $\gamma$  subunit, and the assembly mechanism of the ATP synthase in *Arabidopsis*.

*Loss of the Chloroplast ATP Synthase Causes High Non-photochemical Quenching*—Several ATP synthase mutants in *Chlamydomonas* have been shown to be light-sensitive (54) and the same is true for *dpa1*. As a consequence of the ATP synthase disruption, accumulation of a large electrochemical gradient through the thylakoid membrane that induces qE, the energetic component of NPQ, might be expected (55). Therefore, quenching of the fluorescence was in fact also expected to occur in *Chlamydomonas* ATP synthase mutants. Surprisingly, the major effect in the *Chlamydomonas* mutants is a light intensity-dependent rise of the steady state fluorescence level ( $F_s$ ) up to a level very close to  $F_m$  (54). It has been suggested that  $\Delta\mu_{H^+}$ -dependent NPQ was not induced under the experimental conditions. In contrast, in *dpa1*, increasing light intensity results in increasing NPQ and a drop of  $F_s$  even below the initial dark  $F_0$  level. This difference shows that fluorescence signals and quenching mechanisms differ significantly between the green algae and higher plants. A different extent in the dissipation of excess absorbed light energy has been described

FIG. 8. **mRNA expression profiling of 3292 nuclear genes in *dpa1*.** Total RNA isolated from 3-week-old plants grown under continuous light at a photon flux density of  $20 \mu\text{mol photons m}^{-2} \text{s}^{-1}$  was used. Up- and down-regulated genes were classified in 13 major functional categories. Except for photosynthetic genes the expression of all other classes was strongly down-regulated. The array data were confirmed by Northern analysis with randomly chosen gene probes (see "Experimental Procedures").

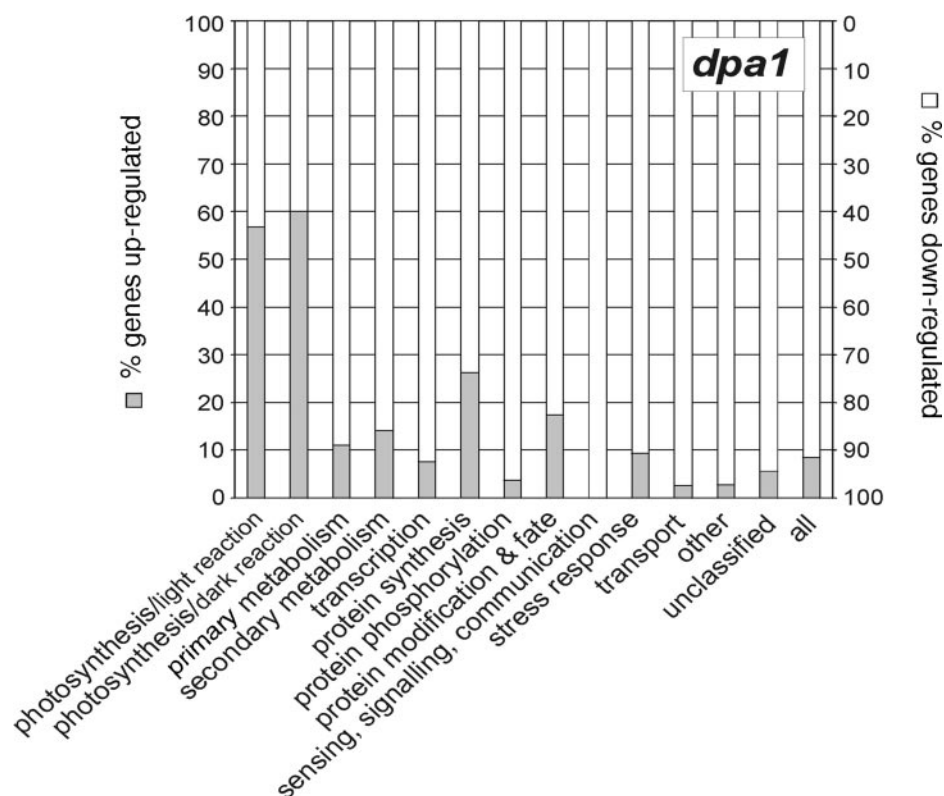


TABLE II  
Representative expression levels of up- and down-regulated nuclear photosynthetic genes in *dpa1*

		Up-regulated		Down-regulated		
	Accession no.	Annotation	Ratio <i>dpa1</i> /WT	Accession no.	Annotation	Ratio <i>dpa1</i> /WT
Electron carrier	At1g20340	PetE2 (plastocyanin)	3.49	At4g14890	PetF5 (ferredoxin)	0.40
				At5g10000	PetF4 (ferredoxin)	0.13
PSI	<i>psaA</i>	PSI-A	3.69			
	At1g55670	PSI-G	2.63			
PSII	At1g79040	PSII-R	2.96	At1g03600	PSII protein family	0.36
	At1g4457	PsbS	2.41	At2g30790	PSII-P2	0.34
	At5g66570	PsbOI	2.17	At4g15510	PSII-P related protein	0.32
	At1g67740	PsbY	1.73	At3g01440	PSII-Q related protein	0.19
	At2g06520	PsbX	1.52			
Cytb6/f	At2g2650	PetM	1.91			
ATP synthase	At4g09650	AtpD	1.37			
	At4g32260	AtpG	1.37			
Dark reaction	At5g38420	Rubisco small subunit 2b	4.92	At1g73110	Putative Rubisco activase	0.36
	<i>rbcL</i>	Rubisco large subunit	4.65	At3g55800	Sedoheptulose-bisphosphatase	0.34
	At5g38430	Rubisco small subunit 1b	4.43	At4g15530	Pyruvate, orthophosphate dikinase	0.23
	At1g67090	Putative Rubisco small subunit	4.23			
	At1g56190	Putative phosphoglycerate kinase	3.73			
	At1g32060	Phosphoribulokinase	2.39			

in respect to the xanthophyll cycle for the *npq* mutants of *Chlamydomonas* and *Arabidopsis* (65, 66). Inactivation of the violaxanthin de-epoxidase results in an impaired NPQ of 25% in *Chlamydomonas* and of 85% in *Arabidopsis*, suggesting a larger contribution of xanthophyll cycle-dependent NPQ in *Arabidopsis* compared with the green alga (66).

**Post-illumination Fluorescence Increase Is Due to Relaxation of Thylakoid Proton Gradient**—We further characterized the fluorescence quenching mechanism and the unusual relaxation that occurs in darkness. Analysis of the relaxation kinetics in the dark allowed us to investigate different factors separately

(Fig. 5). Both far-red light and the measuring beam did not influence the relaxation kinetics of the quenching in the dark. Therefore, the post-illumination fluorescence increase in the dark is not due to reduction of plastoquinone or  $Q_A$ .

In the presence of the uncoupler nigericin strong quenching was abolished in *dpa1* and exciton quenching relaxed when nigericin was applied during fluorescence induction (Fig. 6). These results demonstrate that a low luminal pH causes strong NPQ below the  $F_o$  level in *dpa1*. This is in contrast to the *cfq* mutant that is affected by a decreased  $\Delta\text{pH}$  across the thylakoid membrane due to a higher proton conductivity of the ATP

synthase. Consequently, NPQ was decreased under moderate light intensities in *cfq* (23). High energy quenching as the main component of NPQ (45) depends on low luminal pH and may involve protonation of acidic amino acids on the LHCII polypeptides, in particular PsbS (55, 67). At lower temperatures, formation of zeaxanthin known to be involved in NPQ is slowed down (68). We found that quenching kinetics and relaxation mechanisms in the dark are highly temperature-sensitive in *dpa1*. This suggests that NPQ in *dpa1* is due to the temperature-dependent activity of the violaxanthin de-epoxidase involved in the xanthophyll cycle. Application of the uncoupler nigericin clearly shows that relaxation of quenching in the darkness is due to dissipation of the pH gradient across the thylakoid membrane. Leakage of the membrane increases with increasing the temperature consistently with the temperature-dependent relaxation of quenching. However, we cannot exclude an additional effect of the temperature on the quenching mechanism itself because the biophysical mechanism of chl de-excitation is still unknown (55).

An increased  $F_o$  in *dpa1* results in a reduced ratio  $F_v/F_m$  of  $0.6 \pm 0.05$  as compared with  $0.80 \pm 0.02$  in wild type. This is indicative of disturbances in PSII that might be related to a partial disconnection of the outer antenna or accumulation of reduced  $Q_A$  molecules. Because no ATP formation takes place, electron acceptors in the form of NADP<sup>+</sup> cannot be regenerated, and the photosystems suffer from photoreduction. However, far-red light which excites PSI preferentially was unable even to partially reduce  $F_o$  of dark-adapted plants (data not shown) indicating that the increased  $F_o$  is independent of accumulation of reduced quinones. Moreover, under still moderate light intensities NPQ is able to quench up to 40% of  $F_o$  probably to protect PSII from photodestruction.

Substantial quenching below the initial  $F_o$  fluorescence level during illumination was also observed in several other *Arabidopsis* mutants such as *hcf109* (32, 39) and in a tobacco *psbF* point mutation (69). This quenching also relaxes after switching off actinic light and reaches the  $F_o$  level with similar kinetics to those found in *dpa1*. Because investigation is missing whether far-red light or uncoupling had an effect on the quenching mechanism, it remains to be shown whether the observed dark increase of fluorescence is due to reduction of quinones.

Depending on the light intensity and adverse heat treatment, reductants that accumulate during illumination reduce the plastoquinone pool leading to a transient increase of the fluorescence after light/dark switches (70–74). This reduction depends partially on the activity of the NADH/NADPH-dependent dehydrogenase and can be abolished by application of far-red light. In *dpa1* the fluorescence drops below  $F_o$ , and the relaxation of quenching is not reversible as well as independent from far-red light. Therefore, the post-illumination fluorescence increase in *dpa1* is much different from the above-mentioned phenomena.

**Photoprotective Role of qE**—To identify proteins involved in qE, *Chlamydomonas* and *Arabidopsis* mutants with altered NPQ of chl fluorescence were isolated (66, 75). Two identified genes, *npq1* and *npq2*, are both involved in the xanthophyll cycle, whereas *npq4* encodes the PsbS protein. In *Chlamydomonas* a defect in the chloroplast ATP synthase did not allow a light-dependent increase in qE which leads to fast degradation of PSII (54). Even if PSII is affected in *dpa1* as evidenced by the lower value of  $F_v/F_m$ , no considerable effect on the accumulation of PSII proteins could be observed (Fig. 3). Again, this suggests a protective role of qE on PSII consistent with an increased photoinhibition during short term light stress when qE is impaired (76).

The important role of NPQ in photoprotection implies that NPQ itself has to be modulated in response to rapid changes of physiological conditions (77, 78). Recently, it has been shown that the chloroplast ATP synthase is involved in modulation of NPQ (79). The proton conductivity of the enzyme, as estimated by measurement of the electrochromic shift at 520 nm, is altered at different CO<sub>2</sub> concentrations. This allows the modulation of the relationship between photosynthetic electron transport and NPQ. The *dpa1* mutant represents an extreme example with maximal proton accumulation which only relaxes through leakage of the membrane.

**Up-regulation of Nuclear Photosynthetic Gene Expression in *dpa1***—In the *dpa1* mutant a preferential down-regulation of the differentially expressed genes is observed. A different, and more balanced, response of transcriptional regulation was observed for photosynthetic genes, for which about an equal number of genes were up- or down-regulated. The changes in the accumulation of transcripts for photosynthetic genes could be interpreted as a reaction of the plant to the altered physiological states of thylakoids due to the loss of ATP synthase function. It appears possible that under the conditions induced by the *dpa1* mutation particular components of the photosynthetic apparatus are more rapidly degraded and that as a compensatory response corresponding nuclear genes are up-regulated, e.g. genes of the ATP synthase. On the other hand, up-regulation of genes encoding the cytochrome *b<sub>6</sub>/f* complex, e.g. *petM*, might result in higher levels of this complex (Fig. 3B and Table II).

Another possibility is that certain subunits of the photosynthetic apparatus are down-regulated to decrease the photosynthetic activity of corresponding complexes that could be harmful in the absence of ATP synthase activity. However, a previous comparison of the differential expression of photosynthetic proteins and their transcripts in the *prpl11-1* mutant (48) has shown that complex interdependencies of mRNA and protein levels can occur in photosynthetic mutants. This includes situations where nuclear genes are up-regulated but the levels of corresponding proteins are decreased, due to the interaction of plastome- and nuclear encoded proteins in photosynthetic multiprotein complexes (48). However, taken together, the transcriptional regulation of photosynthetic genes differs from the general trend (Fig. 8), clearly indicating that the plant might be able to monitor the altered photosynthetic state due to loss of ATP synthase activity and to respond by regulating the expression of appropriate photosynthetic genes (see Supplemental Material).

**Acknowledgments**—We are most grateful to Claudia Nickel (München) and Irina Volfson (Düsseldorf) for technical assistance and to Richard J. Berzborn for providing antisera against ATP synthase antibodies. We thank Reinhold G. Herrmann for critical reading of the manuscript.

#### REFERENCES

1. Strotmann, H., Shavit, N., and Leu, S. (1998) *The Molecular Biology of Chloroplast and Mitochondria in Chlamydomonas*, pp. 477–500, Kluwer Academic Publishers, Norwell, MA
2. Groth, G., and Pohl, E. (2001) *J. Biol. Chem.* **276**, 1345–1352
3. Groth, G., and Strotmann, H. (1999) *Physiol. Plant.* **106**, 142–148
4. Nelson, N. (1992) *Curr. Opin. Cell Biol.* **4**, 654–660
5. Ducan, T. M., Bulygin, V. V., Zhou, Y., Hutcheon, M. L., and Cross, R. L. (1995) *Proc. Natl. Acad. Sci. U. S. A.* **92**, 10964–10968
6. Sabbert, D., Engelbrecht, S., and Junge, W. (1996) *Nature* **381**, 623–625
7. Noji, H., Yasuda, R., Yoshida, M., and Kinosita, K. (1997) *Nature* **386**, 299–302
8. Nishio, K., Iwamoto-Kihara, A., Yamamoto, A., Wada, Y., and Futai, M. (2002) *Proc. Natl. Acad. Sci. U. S. A.* **99**, 13448–13452
9. Nalin, C. M., and McCarty, R. E. (1984) *J. Biol. Chem.* **259**, 7275–7280
10. Ketcham, S. R., Davenport, J. W., Warncke, K., and McCarty, R. E. (1984) *J. Biol. Chem.* **259**, 7286–7293
11. Junesch, U., and Gräber, P. (1987) *Biochim. Biophys. Acta* **893**, 275–288
12. Ross, S. A., Zhang, M. X., and Selman, B. R. (1995) *J. Biol. Chem.* **270**, 9813–9818
13. Ort, D. R., and Oxborough, K. (1992) *Annu. Rev. Plant Physiol. Plant Mol. Biol.* **43**, 269–291

14. Selman-Reimer, S., Duke, R. J., Stockman, B. J., and Selman, B. R. (1991) *J. Biol. Chem.* **266**, 182–188
15. Bald, D., Noji, H., Yoshida, M., Hirono-Hara, Y., and Hisabori, T. (2001) *J. Biol. Chem.* **276**, 39505–39507
16. Falk, G., and Walker, J. E. (1988) *Biochem. J.* **254**, 109–122
17. Klionsky, D. J., and Simoni, R. D. (1985) *J. Biol. Chem.* **260**, 11207–11215
18. Wollman, F. A., Minai, L., and Nechushtai, R. (1999) *Biochim. Biophys. Acta* **1411**, 21–85
19. Inohara, N., Iwamoto, A., Moriyama, Y., Shimomura, S., Maeda, M., and Futai, M. (1991) *J. Biol. Chem.* **266**, 7333–7338
20. Legen, J., Misera, S., Herrmann, R. G., and Meurer, J. (2001) *DNA Res.* **8**, 53–60
21. Witt, H. T. (1978) *Biochim. Biophys. Acta* **505**, 355–427
22. Gabrys, H., Kramer, D. M., Crofts, A. R., and Ort, D. R. (1994) *Plant Physiol.* **104**, 769–776
23. Govindjee, and Spilotro, P. (2002) *Funct. Plant Biol.* **29**, 425–434
24. Meurer, J., Meierhoff, K., and Westhoff, P. (1996) *Planta* **198**, 385–396
25. Jander, G., Norris, S. R., Rounsley, S. D., Bush, D. F., Levin, I. M., and Last, R. L. (2002) *Plant Physiol.* **129**, 440–450
26. Reiss, B., Klemm, M., Kosak, H., and Schell, J. (1996) *Proc. Natl. Acad. Sci. U. S. A.* **93**, 3094–3098
27. Clough, S. J., and Bent, A. F. (1998) *Plant J.* **16**, 735–743
28. Hadi, M. Z., Kemper, E., Wendeler, E., and Reiss, B. (2002) *Plant Cell Rep.* **21**, 130–135
29. Steiner, J. J., Poklema, C. J., Fjellstrom, R. G., and Elliott, L. F. (1995) *Nucleic Acid Res.* **23**, 2569–2570
30. Dellaporta, S. L., Wood, J., and Hicks, J. B. (1983) *Plant Mol. Biol. Rep.* **1**, 19–21
31. Sambrook, J., Fritsch, E. F., and Maniatis, T. (1989) *Molecular Cloning: A Laboratory Manual*, pp. 7.1–9.62, Cold Spring Harbor Laboratory Press, Cold Spring Harbor, NY
32. Meurer, J., Lezhneva, L., Amann, K., Gödel, M., Bezghani, S., Sherameti, I., and Oelmüller, R. (2002) *Plant Cell* **14**, 3255–3269
33. Wittwer, C. T., Ririe, K. M., Andrew, R. V., David, D. A., Gundry, R. A., and Balis, U. J. (1997) *BioTechniques* **22**, 176–181
34. Strotmann, H., and Bickel-Sandkötter, S. (1977) *Biochim. Biophys. Acta* **460**, 126–135
35. Strotmann, H., Thelen, R., Müller, W., and Baum, W. (1990) *Eur. J. Biochem.* **193**, 879–886
36. Kothen, G., Schwarz, O., and Strotmann, H. (1995) *Biochim. Biophys. Acta* **1229**, 208–214
37. Schwarz, O., and Strotmann, H. (1998) *Photosynth. Res.* **57**, 287–295
38. Avron, M. (1960) *Biochim. Biophys. Acta* **40**, 257–272
39. Meurer, J., Berger, A., and Westhoff, P. (1996a) *Plant Cell* **8**, 1193–1207
40. Bradford, M. M. (1976) *Anal. Biochem.* **72**, 248–254
41. Blum, H., Beier, H., and Gross, H. J. (1987) *Electrophoresis* **8**, 93–99
42. Meurer, J., Plücken, H., Kowallik, K. V., and Westhoff, P. (1998) *EMBO J.* **17**, 5286–5297
43. Laskey, R. A. (1980) *Methods Enzymol.* **65**, 363–371
44. Swiatek, M., Regel, R. E., Meurer, J., Wanner, G., Pakrasi, H. B., Ohad, I., and Herrmann, R. G. (2003) *Mol. Genet. Genomics* **268**, 699–710
45. Krause, G. H., and Weis, E. (1991) *Annu. Rev. Plant Physiol. Plant Mol. Biol.* **42**, 313–349
46. van Kooten, O., and Snel, J. F. H. (1990) *Photosynth. Res.* **25**, 147–150
47. Nishio, J. N., and Whitmarsh, J. (1993) *Plant Physiol.* **101**, 89–96
48. Kurth, J., Varotto, C., Pesaresi, P., Biehl, A., Richly, E., Salamini, F., and Leister, D. (2002) *Planta* **215**, 101–109
49. Richly, E., Dietzmann, A., Biehl, A., Kurth, J., Laloi, C., Apel, K., Salamini, F., and Leister, D. (2003) *EMBO Rep.* **4**, 491–498
50. Sanger, F., Nicklen, S., Coulson, A. R. (1992) *Bio/Technology* **24**, 104–108
51. Rosenblum, B. B., Lee, L. G., Spurgeon, S. L., Khan, S. H., Menchen, S. M., Heiner, C. R., and Chen, S. M. (1997) *Nucleic Acids Res.* **25**, 4500–4504
52. Murashige, T., and Skoog, F. (1962) *Physiol. Plant.* **15**, 473–497
53. Felmann, K. A. (1991) *Plant J.* **1**, 71–82
54. Majeran, W., Olive, J., Drapier, D., Vallon, O., and Wollman, F. A. (2001) *Plant Physiol.* **126**, 421–433
55. Müller, P., Li, X. P., and Niyogi, K. K. (2001) *Plant Physiol.* **125**, 1558–1566
56. Ross, S. A., Zhang, M. X., and Selman, B. R. (1996) *J. Bioenerg. Biomembr.* **28**, 49–57
57. Konno, H., Yodogawa, M., Stumpp, M. T., Kroth, P., Strotmann, H., Motohashi, K., Amano, T., and Hisabori, T. (2000) *Biochem. J.* **352**, 783–788
58. The Arabidopsis Genome Initiative (2000) *Nature* **408**, 796–815
59. Vision, T. J., Brown, D. G., and Tanksley, S. D. (2002) *Science* **290**, 2114–2117
60. Hadikusumo, R. G., Meltzer, S., Choo, W. M., Jean-François, M. J. B., Linnane, A. W., and Marzuki, S. (1988) *Biochim. Biophys. Acta* **933** 212–222
61. Lemaire, C., and Wollman, F. A. (1989) *J. Biol. Chem.* **264**, 10235–10242
62. Robertson, D., Boynton, J. E., and Gillham, N. W. (1998) *Mol. Gen. Genet.* **221**, 155–163
63. Smart, E. J., and Selman, B. R. (1991) *Mol. Cell. Biol.* **11**, 5053–5058
64. Ackerman, S. H. (2002) *Biochim. Biophys. Acta* **1555**, 101–105
65. Niyogi, K. K., Björkman, O., and Grossman, A. R. (1997) *Plant Cell* **9**, 1369–1380
66. Niyogi, K. K., Grossman, A. R., and Björkman, O. (1998) *Plant Cell* **10**, 1121–1134
67. Gilmore, A. M., Govindjee (1999) in *Concepts in Photobiology: Photosynthesis and Photomorphogenesis* (Singhal, G. S., Renger, G., Sopory, S. K., Irrgang, K.-D., and Govindjee, eds) pp. 513–548, Narosa Publishing House, New Delhi, India
68. Bilger, W., and Björkman, O. (1994) *Planta* **193**, 238–246
69. Bondarava, N., De Pascalis, L., Al-Babili, S., Goussias, C., Golocky, J. R., Beyer, P., Bock, R., and Krieger-Liszay, A. (2003) *J. Biol. Chem.* **278**, 13554–13560
70. Cao, J., and Govindjee, (1990) *Biochim. Biophys. Acta* **1015**, 180–188
71. Havaux, M. (1996) *Photosynth. Res.* **47**, 85–97
72. Sazanov, L. A., Burrows, P. A., and Nixon, P. J. (1998) *FEBS Lett.* **429**, 115–118
73. Yamane, Y., Shikanai, T., Kashino, Y., Koike, H., and Satoh, K. (2000) *Photosynth. Res.* **63**, 23–34
74. Bukhov, N. G., Samson, G., and Carpentier, R. (2000) *Photochem. Photobiol.* **72**, 351–357
75. Li, X. P., Björkman, O., Shih, C., Grossman, A. R., Rosenquist, M., Jansson, S., and Niyogi, K. K. (2000) *Nature* **403**, 391–395
76. Li, X. P., Muller-Moule P., Gilmore, A. M., and Niyogi, K. K. (2002) *Proc. Natl. Acad. Sci. U. S. A.* **99**, 15222–15227
77. Heber, U., and Walker, D. (1992) *Plant Physiol.* **100**, 1621–1626
78. Asada, K. (1996) in *Phytosynthesis and the Environment* (Baker, N. R., ed) Vol. 5, 123–150, Kluwer Academic Publishers Group, Dordrecht, Netherlands
79. Kanazawa, A., and Kramer, D. M. (2002) *Proc. Natl. Acad. Sci. U. S. A.* **99**, 12789–12794